0026-895X/07/7101-344–356$20.00
MOLECULAR PHARMACOLOGY
Copyright © 2007 The American Society for Pharmacology and Experimental Therapeutics
Mol Pharmacol 71:344–356, 2007

Vol. 71, No. 1
24240/3143490
Printed in U.S.A.

Geldanamycin Interferes with the 90-kDa Heat Shock Protein, Affecting Lipopolysaccharide-Mediated Interleukin-1 Expression and Apoptosis within Macrophages

Hsien-Yeh Hsu, Hua-Lin Wu, Sai-Koong Tan, Vivian Pei-Hsin Li, Wei-Ting Wang, Jason Hsu, and Ching-Hsun Cheng

Department of Biotechnology and Laboratory Science in Medicine, National Yang-Ming University, Taipei, Taiwan (H.-Y.H., S.-K.T., V.P.-H.L., W.-T.W., C.-H.C.); Department of Education and Research, Taipei City Hospital, Taipei, Taiwan (H.-Y.H.); Department of Biochemistry and Molecular Biology, College of Medicine, and Cardiovascular Research Center, National Cheng Kung University, Tainan, Taiwan (H.-L.W.); and Stephen M. Ross School of Business, University of Michigan, Ann Arbor, Michigan (J.H.)

Received March 7, 2006; accepted July 6, 2006

ABSTRACT

We have demonstrated that lipopolysaccharide (LPS)-mediated reactive oxygen species (ROS) and signal transduction are involved in the regulation of interleukin-1 (IL-1) β gene expression within macrophages. Because the 90-kDa heat shock protein (Hsp90) plays an important role in the LPS mediation of macrophage activation, using Hsp90 inhibitor geldanamycin A (GA), we analyzed the mechanism of Hsp90 upon LPS-transduced signaling in the regulation of IL-1 expression and determined the function of Hsp90 regarding the viability of human primary macrophages and murine macrophages cell line. In essence, GA decreased LPS-induced Hsp90/pp60Src heterocomplex formation. In addition, Hsp90 is important for IL-1 protein translation, plays a minor role in IL-1 mRNA transcription, and is involved in nuclear factor-κB activation and the phosphorylation and activation of p38, c-Jun NH_2-terminal kinase, and extracellular signal-regulated kinase; however, Hsp90 plays a more important role in LPS-stimulated p38 activation. In analyzing the function of Hsp90 regarding the cytotoxicity/viability of macrophages, we found that the combination of LPS and GA increases apoptosis, as evidenced by the increased caspase-3 activity and the proportion of nuclear/chromatin condensation. In contrast, *N*-acetyl-cysteine dramatically blocked GA/LPS-induced ROS production, simultaneously decreasing caspase-3 activity and the presence of apoptotic nuclei. We concluded that Hsp90 plays an indispensable role in the process of LPS-induced IL-1 secretion. Furthermore, we established the mechanism of GA interference with Hsp90 function for LPS-stimulated macrophages, resulting in increased ROS production and caspase-3 activation, and consequently leading to synergistic enhancement of macrophage apoptosis.

Lipopolysaccharide (LPS, an endotoxin), a potent activator of the human immune system, induces local inflammation and septic shock for severe cases of Gram-negative bacterial infections (Guha and Mackman, 2001). The innate immune responses of macrophages to microorganisms involve toll-like receptors (TLRs), which resist infection and induce signals, including the activation of protein tyrosine kinase, protein kinases, and mitogen activated protein kinases (MAPKs) (Ulevitc and Tobias, 1995; Hsu and Wen, 2002) that inform the adaptive immune system of pathogens (Medzhitov et al., 1997). Thereafter, the MAPK-mediated signals stimulate downstream pathways

This work was supported by National Science Council (NSC), Taiwan (NSC 94-2120-M-010-002 and NSC 93-2314-B-010-003 to H.-Y.H.), National Health Research Institutes, Taiwan (NHRI-EX94-9211SI to H.-Y.H.), NSC 95-2752-B-006-003-PAE (to H.-L.W.), and a grant from the Ministry of Education, Aim for the Top University Plan (95A-C-D01-PPG-10 to H.-Y.H.).

H.-Y.H. and H.-L.W. contributed equally to this work.

Article, publication date, and citation information can be found at http://molpharm.aspetjournals.org.

doi:10.1124/mol.106.024240.

ABBREVIATIONS: LPS, lipopolysaccharide; Hsp90, 90-kDa heat shock protein; TLR, toll-like receptor; IRAK-1, interleukin-1 receptor-associated kinase-1; GA, geldanamycin A; ROS, reactive oxygen species; IL-1, interleukin-1β; pro-IL-1, prointerleukin-1β; NAC, *N*-acetyl-cysteine; NF-κB, nuclear factor-κB; MAPK, mitogen-activated protein kinase; ERK, extracellular signal-regulated kinase; JNK, c-Jun NH_2-terminal protein kinase; p38, p38 mitogen-activated protein kinase; ATF, activating transcription factor; TNF, tumor necrosis factor; FBS, fetal bovine serum; PBMC, peripheral blood mononuclear cell; PBS, phosphate-buffered saline; CTR, control; PMSF, phenylmethylsulfonyl fluoride; HA, herbimycin A; DAPI, 4′,6-diamidino-2-phenylindole; RT-PCR, reverse transcription-polymerase chain reaction; bp, base pair; HRP, horseradish peroxidase; GAPDH, glyceraldehyde phosphate dehydrogenase; MTT, 3-(4,5-dimethylthiazol-2-yl)-2,5-diphenyltetrazolium; PAGE, polyacrylamide gel electrophoresis; DCFH, 2′,7′-dichlorofluorescein diacetate; Src, pp60Src; Ac-DEVD-AMC, *N*-acetyl-Asp-Glu-Val-Asp-amino-4-methylcoumarin; CM-DCFH, carboxyl-2′,7′-dichlorofluorescein diacetate.

in the activation of certain transcription factors, including activator protein-1, NF-κB (Karin, 1995), and ATF-2 (Gray et al., 1993), which, in turn, trigger a battery of genes encoded for inflammatory cytokines such as IL-1, IL-6, and TNF (Karin, 1995; Hsu and Wen, 2002).

Heat shock proteins, including Hsp90, constitute a group of "chaperone" proteins that help to maintain the stability of client proteins and/or target the degradation of unfolded proteins when cells are exposed to heat shock or other kinds of stress (Xu and Lindquist, 1993). Geldanamycin A (GA), a specific antagonist of Hsp90, is one of the benzoquinone ansamycins described as a tyrosine kinase inhibitor (DeBoer et al., 1970). The inhibitory effects of GA upon protein kinase activity and signal transduction molecules are probably due to the inhibition of Hsp90 and result in destabilization and degradation of client proteins (Xu and Lindquist, 1993; Whitesell et al., 1994; Chavany et al., 1996; Hsu et al., 2001). It has been reported that Hsp90 mediates LPS activation of the murine macrophage RAW 264.7 and that GA blocks the LPS-induced nuclear translocation of NF-κB and the expression of TNF (Byrd et al., 1999; Malhotra et al., 2001). Moreover, treatment of the murine macrophages J774 with GA ameliorated the macrophages' response to LPS, an effect which results from GA inhibition of Hsp90 activity, leading to rapid internalization of CD14 receptors and disappearance from membrane surfaces (Vega and De Maio, 2003). Herein we preincubated cells with GA and investigated the involvement of Hsp90 in LPS-treated macrophages; in essence, we examined Hsp90 function in the regulation of IL-1 and the role of Hsp90 in the viability of macrophages upon LPS stimulation.

We demonstrated the important role of LPS-induced reactive oxygen species (ROS), including H_2O_2 production in mediating the activity of MAPK, ERK, JNK, and p38 in the regulation of IL-1 gene expression (Hsu and Wen, 2002). Our current results indicate that LPS activation of H_2O_2 plays a key role in the induction of apoptosis (Jacobson et al., 1997; Nagata, 1997). Caspases, a family of cysteine proteases, seem to be the core of the apoptosis mechanism that is triggered in response to proapoptotic signaling by a set of apoptotic-related proteases (Nagata, 1997; Hoshi et al., 1998; Condorelli et al., 2001). Herein we investigate the function and role of Hsp90 in the generation of LPS-induced ROS, which relate to the induction of caspase-3 activity and the overall cell apoptosis (Kim et al., 2001).

We have demonstrated that GA inhibition is mediated through the impairment of LPS induction of TLR-mediated signaling. Our results further indicate that GA down-regulates the LPS-induced activity of p38, JNK, and ERK. In addition, GA inhibition of LPS-induced NF-κB activation is important for LPS-induced IL-1 gene expression, indicating the critical function of Hsp90 in LPS-transduced signals. In our further analyses of the physiological role(s) of Hsp90, which relate to cell molecular/cellular characteristics such as viability of macrophages, we examined the relative cytotoxicity of LPS, GA, and the combination of LPS and GA to macrophages. Our current results indicate that the combination of LPS and GA acts synergistically to enhance macrophages apoptosis as evidenced by the increased caspase-3 activity, proportion of apoptotic nuclei, and enhanced chromatin condensation of macrophages.

Materials and Methods

Cell Cultures. The murine macrophage cell line J774A.1 (J774A.1 cell) was obtained from American Type Culture Collection (Manassas, VA); propagated in RPMI 1640 medium supplemented with 10% heated-inactivated fetal bovine serum (Hyclone Co., Logan, UT) and 2 mM L-glutamine (Life Technologies, Inc., Carlsbad, CA); and cultured in a 37°C, 5% CO_2 incubator. For individual experiments, cells were seeded 0.5×10^7 in 10-cm plates with 6 ml of medium and were grown to 85% confluence. Before various treatments, cells were starved for 18 h by changing medium without FBS, unless otherwise indicated. In preparation of primary human monocyte-derived macrophages, we followed the previous procedures (Billiet et al., 2005); in brief, human peripheral blood mononuclear cells (PBMCs) were isolated from the blood of healthy persons from the Taiwan Blood Center (Taipei, Taiwan) by a standard density gradient centrifugation at 2500*g* using Histopaque-1077 lymphocyte separation medium from Sigma-Aldrich Co. (St. Louis, MO) for 30 min at room temperature. The cells at the interface were collected and washed three times in cold phosphate-buffered saline (PBS). PBMCs were resuspended in RPMI medium containing 15% FBS at 5×10^6 cells/ml. Then, 1 ml of the cell suspension was dispensed into individual wells of 12-well plates. PBMCs were allowed to adhere for 2 days at 37°C in a 5% CO_2 humidified incubator. Nonadherent cells were removed by gentle washing three times in PBS. The remaining adherent cells, human monocyte-derived macrophages, were then cultured for another 5 days in RPMI medium containing 15% FBS.

Materials. LPS (from *Escherichia coli* 0111:B4), PMSF, HEPES, bovine serum albumin (fraction V), *N*-acetyl-cysteine (NAC, antioxidant), GA (Fig. 1A), herbimycin A (HA), and 4′,6-diamidino-2-phenylindole (DAPI, for DAPI staining) were purchased from Sigma-Aldrich. EGTA, leupeptin, aprotinin, and DNA molecular weight markers were obtained from Boehringer Mannheim Co. (Mannheim, Germany). Immobilon polyvinylidene difluoride membrane was obtained from Millipore Inc. (Bedford, MA). DuPont nonradioactive Western Blot Chemiluminescence Reagent, Renaissance, was purchased from DuPont NEN Research Products Co. (Boston, MA). REZOl C&T was from PROtech Technology Co. (Taipei, Taiwan). GeneAmp RNA PCR kit for RT-PCR amplification was purchased from PerkinElmer Life Science (Branchburg, NJ). GibcoBRL 100-bp DNA ladder was purchased from Life Technologies. 2′-7′Dichlorodihydrofluorescein diacetate was purchased from Molecular Probes (Eugene, OR). The CaspACE Assay System, Fluorometric, was purchased from Promega (Madison, WI). Anti-IL-1 and 3ZD monoclonal anti-human IgG was from National Institutes of Health (Bethesda, MD); anti-p50, anti-p52, anti-p65, anti-p68, and anti-p75 subunits of NF-κB antibodies rabbit IgG against human NF-κB subunits, cross-reaction with corresponding NF-κB of the mouse and rat; anti-rabbit IgG-HRP, anti-mouse IgG-HRP, anti-goat IgG-HRP, and protein A/G plus-agarose were all obtained from Santa Cruz Biotechnology (Santa Cruz, CA). Anti-diphosphorylated ERK, anti-diphosphorylated JNK, anti-diphosphorylated p38, anti-actin, and anti-Hsp90 monoclonal anti-mouse IgG were all purchased from Sigma-Aldrich. p44/42 MAP Kinase Assay Kit, Stress-Activated Protein Kinase/JNK Assay Kit, and p38 MAP Kinase Assay Kit were purchased from Cell Signaling Technology (Beverly, MA). Primers for prointerleukin-1 (pro-IL-1)/IL-1 and glyceraldehyde phosphate dehydrogenase (GAPDH) were synthesized from local MD Bio. Inc. (Taipei, Taiwan).

Cell Viability Assay. Cells were seeded into triplicate wells at 2.5×10^5 cells/90 μl/well in 96-well plates and were grown for 18 h. Cells were then exposed to various concentrations of GA for 1 h, followed by treatment with LPS for additional 18 h. After all, the MTT assay (3-[4,5-dimethylthiazol-2-yl]-2,5-diphenyltetrazolium bromide; Thiazolyl blue, Cell Proliferation Assay, from Sigma-Aldrich) was performed according to the manufacturer's instructions. In brief, after 18-h LPS treatment, 10 μl of MTT dye (0.5 mg/ml) was added directly to the 96-well plates containing growing cells with 90 μl of medium. The tested cells were incubated for 2 h at

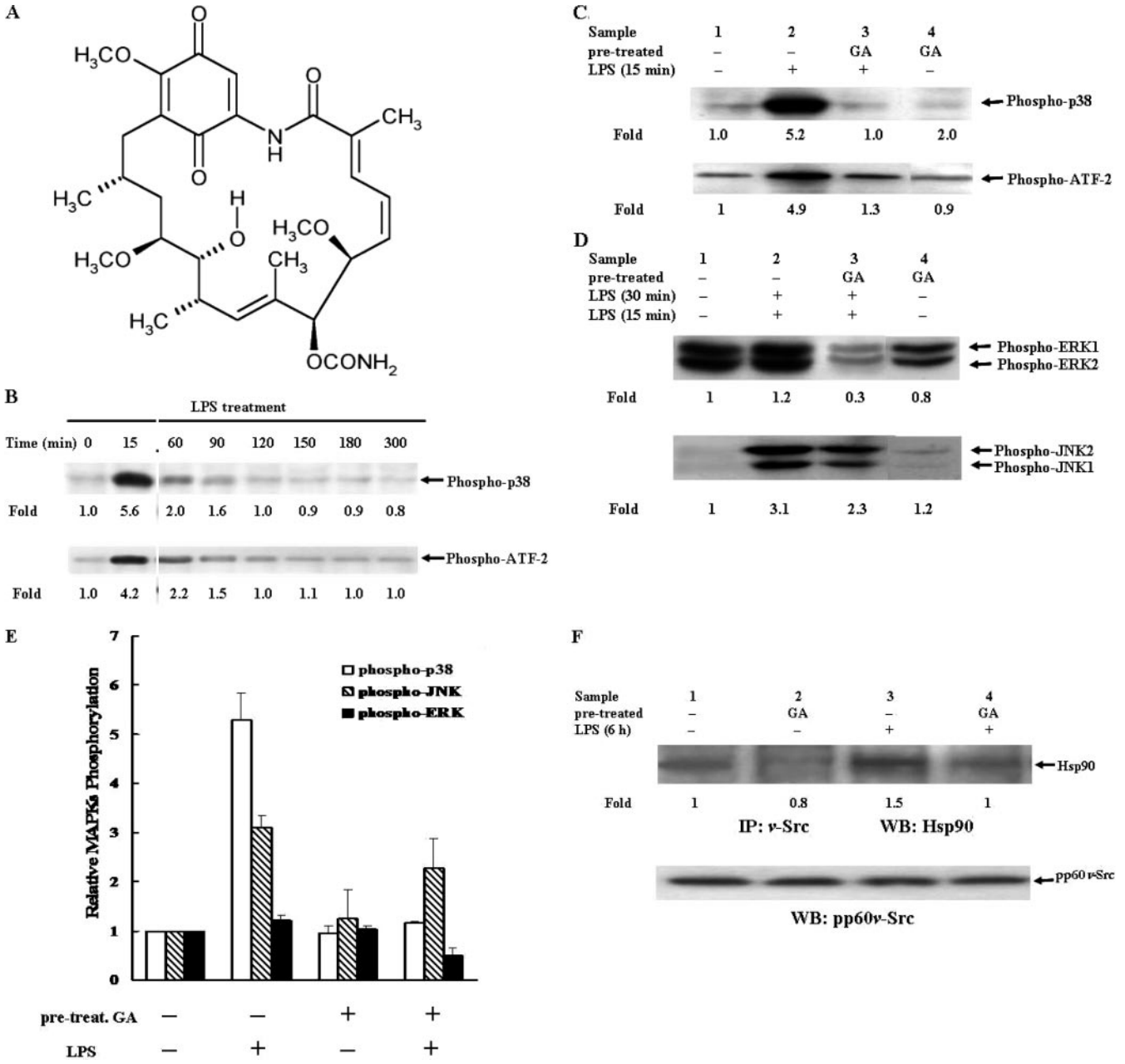

Fig. 1. Effects of GA on LPS-induced MAPK phosphorylation and activity, and GA decreased LPS-induced Hsp90/pp60Src heterocomplex formation in J774A.1 cells. A, structure of geldanamycin A. B, the time course of LPS-induced p38 phosphorylation and LPS-induced p38 activity. Cells (1×10^7 cells/6 ml medium/100-mm plate) were stimulated with LPS (1 μg/ml), and the cell lysates were collected after stimulation at the time indicated. Cell lysates (100 μg of protein) were analyzed by Western blotting with anti-diphosphorylated p38 monoclonal antibody at a position of 38 kDa as described under *Materials and Methods*. The experiments were conducted three times and were from a similar representative experiment ($n = 3$). In addition, the p38 activity in the immunoprecipitant as source of kinase was immunoprecipitated from cell lysates, and the in vitro kinase assays were performed as described previously (Hsu et al., 2001). LPS-induced p38 activity was monitored by phosphorylation of the specific substrate, a recombinant ATF-2 fusion protein, which measured by quantitative immunoblotting with phospho-ATF-2 (Thr71) antibody. The data expressed are from one of three representative experiments. The effects of GA on LPS induction of p38 phosphorylation, p38 activity, ERK phosphorylation (C), and JNK phosphorylation (D). Cells (1×10^7 cells/6 ml medium/100-mm plate) were incubated with GA (0.5 μM) for 60 min before 15- or 30-min LPS (1 μg/ml) stimulation, and the cell lysates were prepared after stimulation. Cell lysates were analyzed by Western blotting with specific antidiphosphorylated monoclonal antibody for p38, JNK, ERK, and phospho-ATF-2 (Thr71) antibody for p38 activity as described under *Materials and Methods*. Data of increased or decreased -fold were expressed in comparison with untreated cells (i.e., -fold of control untreated cells defined as 1). Three separate experiments were conducted, and the data shown are from one similar representative experiment ($n = 3$). E. Histograms of comparison and quantitative analysis of LPS-induced phosphorylation of p38, JNK, and ERK. The values shown are the mean ± S.E. Data of increased or decreased phosphorylation are expressed in comparison with untreated cells (i.e., -fold of phosphorylation in control untreated cells defined as 1). The results are from one of three similar independent experiments ($n = 3$). F, cells were preincubated with GA (0.5 μM) for 60 min followed by 6 h of LPS (1 μg/ml) treatment. Cell lysates were immunoprecipitated with monoclonal anti-pp60Src IgG at 4°C for 4 h, and immunocomplexes were recovered via incubation with protein A/G plus agarose at 4°C for 24 h. Immunoprecipitates were separated by SDS-polyacrylamide gel electrophoresis and immunoblotted with monoclonal anti-Hsp90 IgG protein visualization on each immunoblot was performed with Renaissance Western blot chemiluminescence reagent as described previously. Results were obtained in three separate experiments. The pp60Src immunoblots (internal control for immunoprecipitates and protein loading) are indicated as arrows on the right-hand side. All data of relative increased -fold is expressed compared with untreated J774A.1 cells (i.e., $t = 0$, fold of control cells defined as 1). These figures are representative of three independent experiments.

37°C, and the converted dye was solubilized with acidic isopropanol (0.04–0.1 N HCl in absolute isopropanol). Absorbance of converted dye is measured at a wavelength of 570 nm with background subtraction at 630 to 690 nm.

Reagents for Electrophoresis Mobility Shift Assay. NF-κB binding sequence was from Life Technologies; T4 polynucleotide kinase was from New England BioLabs, Inc. (Beverly, MA); poly(dI-dC), β-mercaptoethanol, and Nonidet P-40 were from Sigma-Aldrich.

RNA Isolation, RT, and PCR Amplification for pro-IL-1/IL-1 Expression, Western Blotting Analysis, Assays of Phosphorylation, and Kinase Activity of ERK, JNK, p38, and Enzyme-Linked Immunosorbent Assay for IL-1. All methods and procedures followed the previous descriptions (Hsu and Wen, 2002).

Measurement of NF-κB Activation by Electrophoretic Mobility Shift Assay and SuperShift Assay. Electrophoretic mobility shift assay (EMSA) was carried out as described previously (Delude et al., 1994). In brief, the tested cells (1×10^7 cells per treatment) were harvested and suspended in 700 μl of a hypotonic solution of 1 M HEPES, pH 7.9, 1 M $MgCl_2$, and 1 M KCl, with PMSF and DTT added to 0.5 mM just before use, on ice for 5 min. Cells were centrifuged at 10,000*g* on a Hettich Universal 30RF centrifuge with a 1412 rotor for 5 min at 4°C, and the pellet of nuclear fraction was collected. The nuclear fraction was resuspended in a buffer containing 1 M HEPES, pH 7.9, 1 M NaCl, 1 M $MgCl_2$, 25% glycerol, and 0.25 M EDTA, with PMSF and DTT added to 0.5 mM, rotated at 4°C for 30 min, and centrifuged at 16,000*g* on a microcentrifuge for 10 min at 4°C. The crude nuclear proteins in the supernatant were collected and stored at −70°C for the subsequent EMSA experiments. Two synthetic oligonucleotides (purchased from Life Technologies) containing the NF-κB binding sequence of the murine immunoglobulin light chain gene (5′-GATCCAAGGGGACTTTCCATGGATCCAAGGGGACTTTCCATG-3′) and the complementary sequence (3′-GTTCCCCTGAAAGGTACCTAGGTTCCCCTGAAAGGTACCTAG-5′) were end-labeled by using [γ-^{32}P]dATP and T4 polynucleotide kinase from New England BioLabs. A 5- to 10-μg sample of nuclear protein was incubated with 20 to 25 μl of incubation buffer and mixed on ice for 15 min before the addition of labeled DNA probe (approximately 50,000–100,000 cpm/0.1 ng). Reaction was performed at room temperature for 20 min, and then the reaction mixture was applied to a 6% native PAGE. After electrophoresis, the gel was dried, and an autoradiogram was obtained using a PhosphorImager Model Storm 840 (Molecular Dynamics, Little Chalfont, Buckinghamshire, UK). To confirm specific binding of labeled oligonucleotides to the nuclear protein, an excess amount of unlabeled oligonucleotide (2 ng) was added to the reaction mixture, and the disappearance of the shifted band was examined. An unrelated oligonucleotide (20 ng) corresponding to human PRDI-BF1 was used as a nonspecific control (Zhang and Ghosh, 2001). For supershift assay, the nuclear extract was incubated with 2 μg of anti-p50, ant-p52, anti-p65, anti-RelB (p68), and anti-c-Rel (p75) subunits of NF-κB antibodies, respectively, and the labeled oligonucleotide for 15 min. The reaction mixtures were subjected to electrophoresis on a 6% native PAGE.

Measurement of LPS-Induced ROS. LPS-stimulated ROS was measured by detecting the fluorescent intensity of either 2′,7′-dichlorofluorescein diacetate (DCFH) oxidized product, DCF, or the improved carboxyl-DCFH (CM-DCFH) (Molecular Probes) as described previously (Wan et al., 1993; Hsu and Wen, 2002). For the treatment of the antioxidant NAC, cells were pretreated with NAC (10 mM) for 20 min before LPS stimulation, and the ROS measurement was as indicated.

Detection of Apoptotic Cells with DAPI Staining. Cells were seeded at a concentration of 1.2×10^5/ml, and 3 ml of cell suspension was dispensed into each well of six-well plates. After 18 to 24 h of incubation, cells would adhere and grow on amino acid-like polylysine-coated slides (Mazia et al., 1975) followed by various treatments as indicated. At the end of the experiments, cells were washed with 1 ml of PBS three times, and then cells were stained with 10 μg/ml DAPI for 30 min. The plates were washed with PBS three times and examined under a fluorescent microscope (Jacobson et al., 1997).

Caspase-3 Activity Assay. The measurement of caspase-3 activity in cells basically was described as the protocol from the CaspACE Assay System Fluorometric (Promega). In brief, cells were pretreated with NAC (10 mM) and GA (0.5∼1 μM) for 20 and 60 min, respectively, followed by incubation with LPS (1 μg/ml) for the desired times. At the indicated time, cells were washed twice with ice-cold PBS (without Ca^{2+} and Mg^{2+}), harvested in 100 μl of cell suspension buffer (25 mM HEPES, pH 7.5, 5 mM $MgCl_2$, 5 mM EDTA, 5 mM DTT, 2 mM PMSF, 10 μg/ml pepstatin A, and 10 μg/ml leupeptin). The suspended cells were stored in 1.5-ml centrifuge tubes, frozen and thawed three times, and then centrifuged at 12,000*g* at 4°C for 15 min; the supernatant of each tube was saved, and the pellet was discarded. The protein concentration of supernatant was then determined, and the rest was saved at −80°C freezer for future use. For assaying caspase-3 (CPP32) activity, 32 μl of enzyme assay buffer (2 μl of dimethyl sulfoxide and 10 μl of 100 mM DTT) was added to cell supernatant (containing 75 μg of protein) of the tested sample and then adjusted with distilled water to 98 μl; for each tested sample, a blank control (32 μl of enzyme assay buffer, 2 μl of dimethyl sulfoxide, 10 μl of 100 mM DTT, and 54 μl of distilled water) was also prepared. All of the tested samples were incubated at 30°C for 30 min, and then 2 μl of 2.5 μM CPP32 substrate (Ac-DEVD-AMC) was added to each tested sample, and an additional incubation was conducted at 30°C for 60 min. The intensity of fluorescence for each tested sample was measured at excitation wavelength 360 nm, emission wavelength 460 nm. Caspase-3 activity of the tested sample is correlated with the concentration of free AMC generated in the reaction. Data were presented as the -fold of activation relative to vehicle-treated control samples.

Statistical Analysis. Statistical differences between the experimental groups were examined by analysis of variance, and statistical significance was determined at $p < 0.05$. The experiments were conducted three times or as indicated, and all data are expressed as mean ± S.E.

Results

Effects of GA upon LPS-Induced Phosphorylation of MAPKs in Murine Macrophage J774A.1 Cells. Our previous studies have shown that the LPS-mediated p38 pathway plays a more important role than the MAPK pathways of JNK and of ERK in the context of the LPS regulation of pro-IL-1/IL-1 (Hsu and Wen, 2002). To investigate the role of Hsp90 involved in LPS-induced signal transduction, we investigated the effect of GA (Fig. 1A) upon the LPS-stimulated phosphorylation of p38, JNK, and ERK. A time-course study of LPS-induced phosphorylation of p38 was performed by using Western blotting with an antibody directed against diphosphorylation of p38, and in addition, an in vitro p38 kinase activity assay was performed by using anti-phospho-ATF-2, an antibody that specifically recognizes the activated threonine 71-phosphorylated form of ATF-2. After LPS stimulation, the time courses for p38 phosphorylation and p38 activity were studied. At 15 min after LPS stimulation, both p38 phosphorylation and p38 activity reached a maximum level of approximately 6- and 4-fold, respectively, compared with the untreated control cells; although after approximately 120 min, they returned to the basal level (Fig. 1B). Next, to test the effects of GA upon p38 phosphorylation and p38 activity, we undertook certain experimentation, the resultant data from which revealing that GA completely abolishes LPS-induced p38 phosphorylation, reducing p38 activ-

ity to the basal level (Fig. 1C). Second, we examined the role of GA in LPS-induced JNK and ERK phosphorylation. Both ERK phosphorylation and activity of JNK and of ERK peaked approximately 30 min after LPS treatment (Hsu and Wen, 2002). The phosphorylation level of JNK for LPS-treated cells was 3-fold greater than the corresponding figure for untreated control cells, whereas in contrast, GA reduced the level of LPS-induced JNK phosphorylation by approximately 30%, although GA alone did not seem to affect the level of JNK phosphorylation. Furthermore, we examined the effect of GA on LPS-induced ERK phosphorylation, and we noted no significant effect of LPS on the level of ERK phosphorylation. In contrast, the level of ERK phosphorylation for GA-treated cells registered as a slight decrease (to approximately 80%) of the level for untreated cells or for LPS-treated cells (Fig. 1D). On the other hand, GA registered a rather large decrease (approximately 70%) in the level of LPS-induced ERK phosphorylation compared with the control. A summary of the results of a comparison between and a quantitative analysis of LPS-induced p38, JNK, and ERK phosphorylation is presented by histogram in Fig. 1E.

GA Decreases LPS-Induced Hsp90/pp60Src Heterocomplex Formation in J774A.1 Cells. It has been reported previously that GA interferes with the formation of a complex between Hsp90 and several tyrosine kinases and signal-transduction molecules (Xu and Lindquist, 1993). To examine the association between Hsp90 and pp60Src (Src) upon LPS stimulation, J774A.1 cells were pretreated with GA for a period of 1 h followed by incubation with LPS for a period of 6 h. Cell lysates were subsequently immunoprecipitated with monoclonal anti-pp60Src IgG, and immunocomplexes were recovered via incubation with protein A/G plus agarose. Immunoprecipitates were separated by SDS-PAGE and then immunoblotted with monoclonal anti-Hsp90 IgG. We demonstrated that LPS induces a complex formation between Src and Hsp90; in contrast, the presence of GA disrupted the LPS-induced complex of Src and Hsp90 formation (Fig. 1F). Thus, it may be that the GA-elicited reduction in the level of LPS-induced Src/Hsp90 complex may disturb LPS-mediated Src or other related downstream signaling mechanisms (see the following sections).

Effects of GA on LPS-Induced IL-1 Gene Expression within Macrophages. Initially, using enzyme-linked immunosorbent assay to measure the concentration of LPS-induced IL-1 in the conditioned media from treatments of LPS and GA plus LPS, we observed that LPS quickly stimulated and increased IL-1 secretion. Specifically, the concentration of LPS-induced IL-1 was approximately 40 and 300 pg/ml, respectively, at 4 and 24 h subsequent to LPS stimulation (Fig. 2A). In contrast to this, however, in the presence of GA, the LPS-induced IL-1 secretion was dramatically reduced to a level of less than 10% of the untreated samples (i.e., 3 pg/ml at 3 h and 20 pg/ml at 24 h) (Fig. 2A). Such results indicate that Hsp90 is involved in the LPS-induced secretion of IL-1. Likewise, pretreatment of GA decreased the LPS-induced TNF expression (data not shown), as has been reported previously (Vega and De Maio, 2003).

To further investigate the molecular mechanism by which GA inhibits IL-1 secretion (molecular mass, 17–18 kDa) in the presence or absence of GA, the LPS-induced IL-1 precursor pro-IL-1 was detected by Western-blotting analysis using an anti-IL-1 monoclonal antibody (National Institutes of Health, Bethesda, MD). Time-course studies for the inhibitory effect of GA upon LPS-induced pro-IL-1 protein production were conducted using J774A.1 cells. As revealed in Fig. 2B, LPS induced a 4-fold pro-IL-1 protein expression at 4 h subsequent to LPS exposure, compared with the control, and this expression peaked at 8 h subsequent to LPS addition (producing a 5-fold increase in expression). After this, the pro-IL-1 protein began to decrease, starting from approximately 12 h after LPS and gradually returning to the basal level at approximately 24 h. To further examine the effect of GA upon LPS-induced pro-IL-1 protein, macrophages were preincubated with GA followed by LPS treatment. As indicated in Fig. 2B, GA completely inhibited LPS-induced pro-IL-1 protein during all experimental periods, a result that seems consistent with the lower level of IL-1 secretion occurring within GA-treated cells (Fig. 2A). These results indicate that Hsp90 plays a critical role in the regulation of pro-IL-1 protein production. A similar result was observed regarding GA inhibition of LPS-induced pro-IL-1 protein for human blood-derived macrophages (Fig. 2C). After this, to examine the role of Hsp90 in LPS-induced pro-IL-1 expression, we investigated the effect of various concentrations (as a dose-response effect) of GA and HA (another Hsp90 destabilizer) upon LPS-induced pro-IL-1 protein production. As illustrated in Fig. 2D, GA inhibited LPS-induced pro-IL-1 production in a dose-dependent manner, and LPS induced pro-IL-1 production, decreasing to approximately 20% of the control pro-IL-1 protein level after exposure to HA and to the basal level appearing at HA concentrations of, respectively, 0.1 and 1 μM (samples 3 and 5 versus samples 1 and 2). By contrast, HA decreased to ~50% of the control pro-IL-1 protein level and to the basal level at HA concentrations of 0.1 and 5 μM, respectively (samples 4 and 8 versus samples 1 and 2). These results indicate that Hsp90 plays a critical role in the regulation of pro-IL-1 protein.

Moreover, using RT-PCR, we further investigated the effect of GA upon LPS-induced pro-IL-1/IL-1 message expression at a transcriptional level. As revealed in Fig. 2E, at 3 h after LPS stimulation, LPS addition resulted in a 5-fold increase in pro-IL-1/IL-1 mRNA expression (sample 2) compared with the untreated control cells (CTR, sample 1) and the GA-treated cells (samples 5–7). At approximately 6 and 12h after LPS stimulation (samples 3 and 4), the LPS-induced pro-IL-1 mRNA level began to gradually decline. In contrast, GA decreased LPS-induced pro-IL-1/IL-1 mRNA expression to a figure of less than 40% of the figure for the mRNA of LPS-stimulated cells (Fig. 2E, samples 2–4 versus samples 8–10).

GA Inhibits LPS-Induced NF-κB Activation. LPS induces the activation of NF-κB and regulates the secretion of TNF, IL-1, and other inflammatory cytokines (Tak and Firestein, 2001; Zhang and Ghosh, 2001). The inflammatory stress response of J774A.1 cells to LPS prompted us to investigate the role of Hsp90 in LPS-induced NF-κB activation. Initially, we investigated whether LPS induces NF-κB activation within J774A.1 cells, and in addition, we tested whether GA decreases LPS-induced IL-1 expression (Fig. 2) as a partial result of the inhibition of LPS-induced NF-κB activation. As indicated in Fig. 3A, the extent of LPS-induced NF-κB activation was extended compared with the control, as evidenced by the following incubation times: at 1, 2, and 4 h after LPS exposure, NF-κB was, respectively, 3-, 6-, and 9-fold the corresponding value for the untreated control

group (Fig. 3A, samples 4, 7, and 10 versus sample 1). In contrast, for GA-pretreated cells subsequently stimulated by LPS incubation, LPS-induced NF-κB activation decreased to 30, 25, and 20% of control values, respectively, at 1, 2, and 4 h after LPS stimulation (Fig. 3A, samples 2 versus 4, samples 5 versus 7, and samples 8 versus 10). These results suggested that GA pretreatment decreased LPS-induced NF-κB activation, results which seem to be quite similar to those of previous reports (Byrd et al., 1999; Vega and De Maio, 2003). In the absence of LPS, GA stimulated NF-κB activity only slightly compared with control cells (samples 1 versus 3). Furthermore, to identify the particular subunit of NF-κB involved in LPS-induced signaling processes, various antibodies for NF-κB subunits were used and examined. As shown in Fig. 3B, the indicated upper band is the supershift pattern of the p65/p50 heterodimer, and the lower bands reveal the presence of the p65/p50 heterodimer and the p50/p50 homodimer.

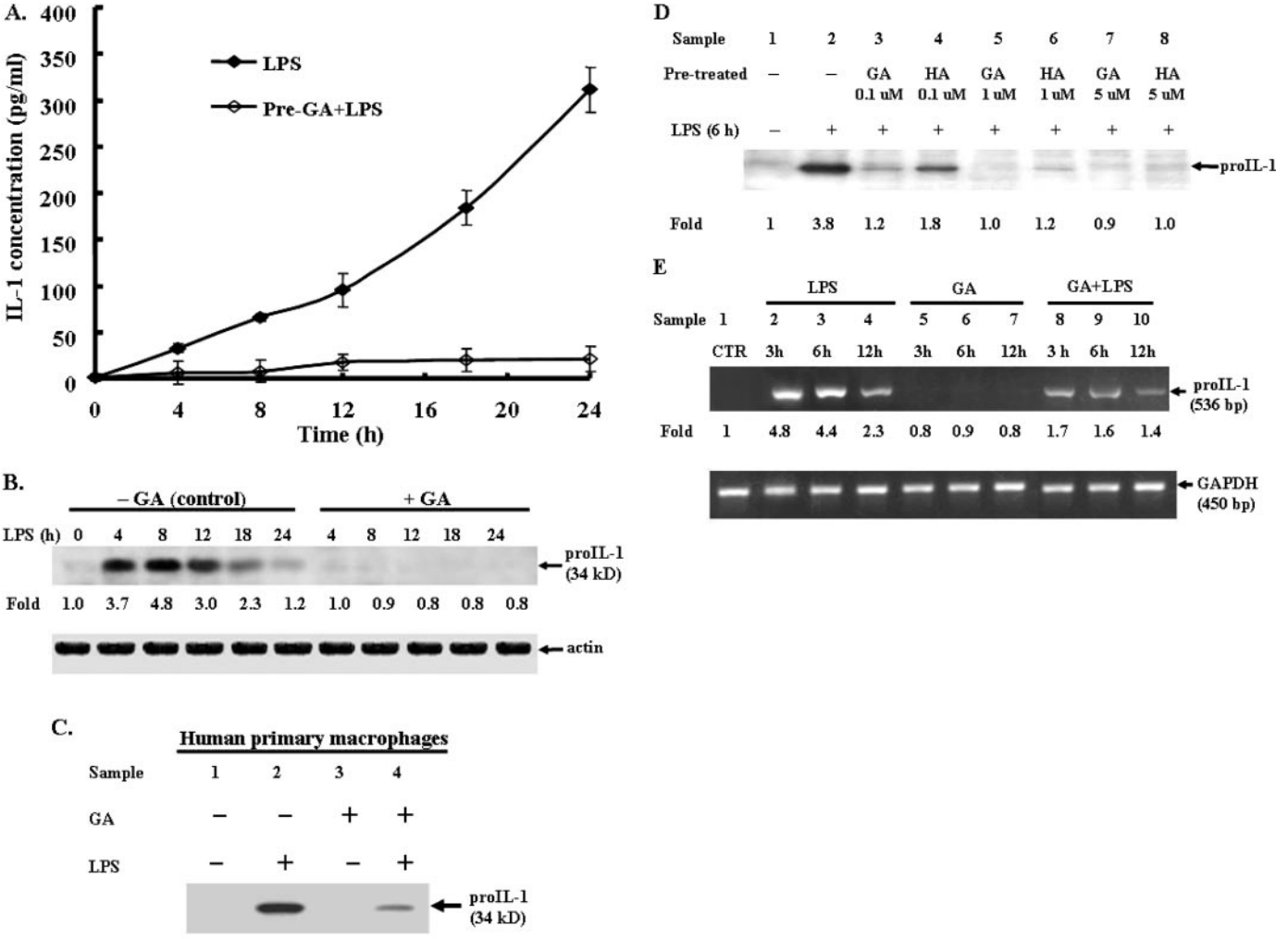

Fig. 2. Effect of GA on LPS-induced pro-IL-1/IL-1 expression in J774A.1 cells. A, time course and the inhibitory effect of GA on LPS-induced IL-1 secretion. J774A.1 cells (1×10^7 cells/6 ml medium/100-mm plate) were preincubated with or without GA (0.5 μM) for 60 min before LPS (1 μg/ml) stimulation, and then the supernatants were collected after stimulation at the time indicated. The IL-1 content in samples was assayed in an IL-1-specific enzyme-linked immunosorbent assay as described under *Materials and Methods*. The experiments were conducted independently four times, and all data were expressed as mean ± S.E. B, time course and the inhibitory effect of GA (0.5 μM) on LPS-induced pro-IL-1 protein production. Cells were stimulated at the indicated time interval, and cell lysates were collected and analyzed by Western blotting analysis with anti-IL-1 monoclonal antibody at a position of 34 kDa for pro-IL-1 protein. Pro-IL-1 and actin (an internal control for protein loading) are indicated as arrows on the right-hand side. All data of altered fold of pro-IL-1 were expressed compared with control untreated J774A.1 cells (i.e., pro-IL-1 of control untreated cells defined as 1), and one of four similar experiments is presented ($n = 4$). C, GA decreased LPS-induced pro-IL-1 protein in human blood monocyte-derived macrophages. Human macrophages (~3×10^6 cells/6 ml medium/100-mm plate) were isolated from the blood of healthy persons by Histopaque-1077 method as described previously (Hsu and Wen, 2002). The treatment and measurement of pro-IL-1 protein were similar to those described in B. D, the effect of various concentrations (does-response) of GA and HA on LPS-induced pro-IL-1 protein production. Cells were pretreated with various concentrations of GA and HA for 60 min before LPS (1 μg/ml) stimulation for 6 h. Cell lysates were collected and analyzed by Western blotting with anti-IL-1 monoclonal antibody at a position of 34 kDa for pro-IL-1 protein. All data of altered fold of pro-IL-1 were expressed compared with control untreated J774A.1 cells (i.e., pro-IL-1 of control untreated cells defined as 1). The figure is one of four similar independent experiments. E, time course and the inhibitory effect of GA on LPS-mediated pro-IL-1/IL-1 mRNA expression. Total RNA was isolated from treated or untreated J774A.1 cells as indicated. Ethidium bromide-stained agarose gel with pro-IL-1 at 536 bp and normalized by comparison with RT-PCR of mRNA of GAPDH gene (450 bp). Arrows indicate RT-PCR products of pro-IL-1 and GAPDH, respectively. The results shown are representative of four independent experiments. Quantification of protein and mRNA expression was carried out by PhosphorImager of each sample using ImageQuant software (Molecular Dynamics), which was expressed as fold increase relative to the level of cells without LPS treatment ($t = 0$, activity of control cells defined as 1).

Effect of GA upon LPS-Induced ROS Production. We have demonstrated previously that LPS rapidly stimulates the release of ROS, including H_2O_2 within macrophages (Hsu and Wen, 2002). Herein, we attempt to further investigate the effect of GA upon LPS-induced H_2O_2 production, with the fluorescent oxidative products of CM-DCFH being detected to examine cell oxygen bursts. As illustrated in Fig. 4, A and B, either GA or LPS induced an enormous H_2O_2 production for, respectively, a short period (0~15 min) and a longer period (0~180 min); moreover, pretreatment of macrophages with GA enhanced LPS-induced H_2O_2 production by 35% compared with only LPS stimulation of cells. The effect of GA pretreatment upon LPS stimulation of macrophages was to elicit an increase in the production of H_2O_2, which continued for up to 180 min (Fig. 4B). In contrast, pretreatment of macrophages with NAC (10 mM), a potent antioxidant, quickly reduced GA/LPS-induced ROS release by approximately 50% compared with the control (Fig. 4A). The difference in GA/LPS-induced ROS production for cells treated

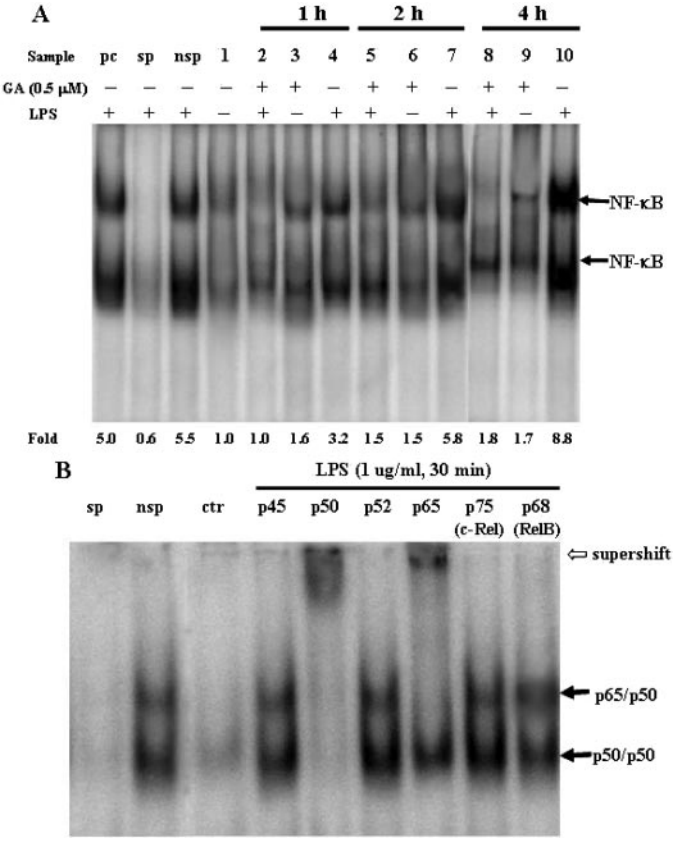

Fig. 3. Effect of GA on LPS-induced NF-κB activation in J774A.1 cells. A, EMSA detection of the effect of GA on LPS-induced NF-κB activation. Cells (1×10^7) were cultured in 10% FBS containing medium with GA (0.5 μM) for 1 h followed by LPS (1 μg/ml) treatment at indicated times. Nuclear proteins were extracted, and 5 μg of each sample was subjected to EMSA using NF-κB consensus site γ-^{32}P-radiolabeled probes. Various treatments were as follows: for positive control cells (pc), cells were treated with LPS for 1 h; for cells with the specific treatment (sp), cells were preincubated with nuclear proteins containing a 50-fold concentrated respective unlabeled probe, which performed the specificity of binding of NF-κB to the DNA; for nonspecific cells (nsp), cells were preincubated with nuclear proteins containing 200-fold concentration of unlabeled probe (PRDI-BFI) to indicate the nonspecificity of binding of NF-κB to the DNA; in sample 1, control cells (ctr) were with no treatment; in sample 2, cells were treated with GA/LPS for 1 h; in sample 3, cells were treated with GA for 1 h; in sample 4, cells were treated with LPS for 1 h; in sample 5, cells were treated with GA/LPS for 2 h; in sample 6, cells were treated with GA for 2 h; in sample 7, cells were treated with LPS for 2 h; in sample 8, cells were treated with GA/LPS for 4 h; in sample 9, cells were treated with GA for 4 h; and in sample 10, cells were treated with LPS for 4 h. Complexes of NF-κB with the labeled DNA were visualized by autoradiography, and the right-side arrow indicates NF-κB complexes. The specificity of binding of NF-κB protein and radiolabeled NF-κB probes was demonstrated by the competition with an unlabeled, identical oligonucleotide but not with unrelated, nonspecific oligonucleotide and was absent with nuclear extracts from unstimulated control cells. B, identity of the subunit components of NF-κB in the EMSA supershift assays. Cells (1×10^7) were cultured in 10% FBS medium containing LPS (1 μg/ml) for 30 min, and the nuclear extract proteins were extracted. Antibodies against NF-κB subunits p45, p50, p52, p65, RelB, (p68) and c-Rel (p75), respectively, were pretreated with nuclear extract proteins for 20 min followed by incubation of the γ-^{32}P-labeled oligonucleotide probes. Complexes of NF-κB were visualized by autoradiography, and the right-side arrow indicates complexes of p65/p50 and p50/p50, respectively; the open arrow shows the supershifted band. The pictures expressed are from one of four representative experiments ($n = 4$).

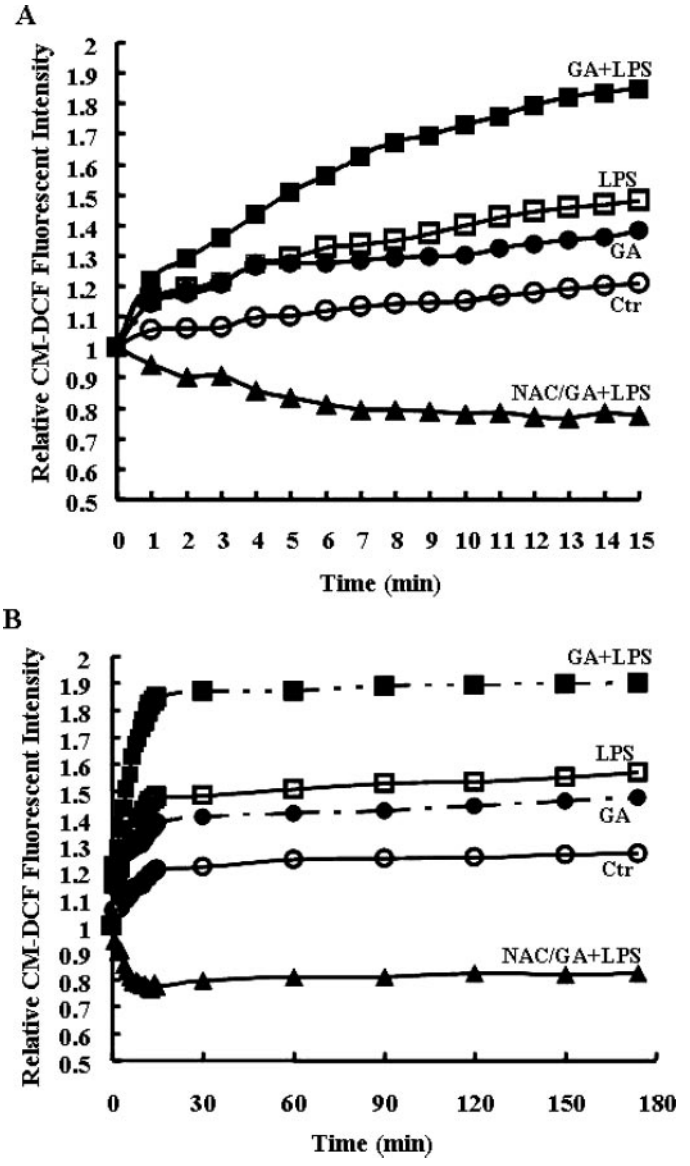

Fig. 4. Effect of GA on LPS-induced release of ROS in J774A.1 cells. To detect the release of ROS, cells were preincubated with CM-DCFH (2 μM), NAC (10 mM), and GA (0.5 μM) for 1 h, followed by substitution with medium containing LPS (1 μg/ml) for additional incubation at the indicated times. The relative fluorescent intensity of fluorophore CM-DCF was detected as described previously (Hsu and Wen, 2002). LPS-induced release of ROS over a short period between 0 and 15 min (A) and over a long period between 0 and 180 min (B).

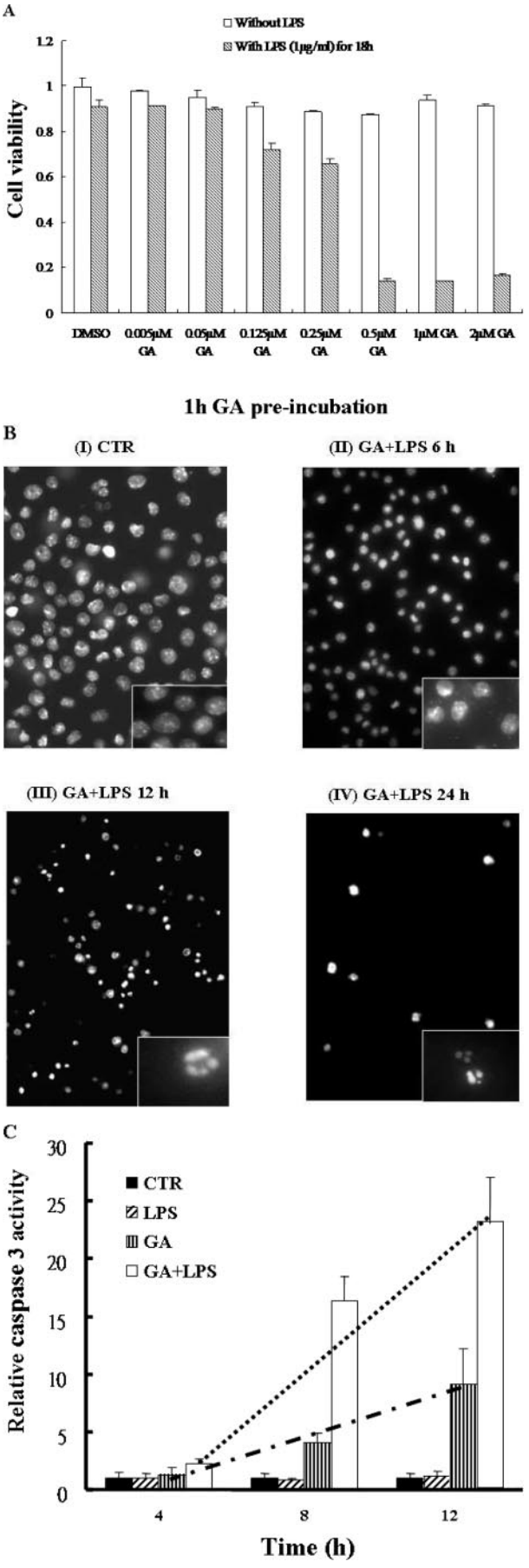

with or without NAC continued for a period of up to 180 min (Fig. 4B).

Combination of GA and LPS Treatment Induces Macrophage Apoptosis. Hsp90 plays an important role in refolding certain denatured proteins, including signaling protein kinases released under stress conditions, and its presence is essential for the viability of various cells (Richter and Buchner, 2001). To examine the effect of GA and LPS on macrophages regarding its impact upon macrophage viability, initially, in the presence of LPS, we used MTT assay to perform the experiments of effect of GA dosage on cultured J774A.1 cell viability. The concentration of GA increased to or greater than 0.5 μM, and the treatment of GA/LPS combination dramatically decreased cell viability to 20% of control cells as detected by MTT (Fig. 5A). Time-course studies (0~24 h) for the effect of GA (at 0.5 μM) upon LPS-induced macrophage viability were conducted. We found that there was no significant difference of cell viability within 4 h while increasing cell death at 8, 12, and 24 h, respectively, after treatment of GA/LPS combination (data not shown; see next sections regarding apoptosis, Fig. 5B, and caspase 3, Fig. 5C).

Next, we investigated cell apoptotic reactions, including nuclear (chromatin) condensation and caspase-3 activation. Any nuclear condensation present was detected by the fluorescent DNA-DAPI staining method (Jacobson et al., 1997). After the treatment of macrophages with GA and LPS, cells were observed at 6, 12, and 24 h after treatment with LPS. At such times, adherent cells on polylysine-coated slides were collected, after which they were stained with DAPI and then inspected under a fluorescent microscope to observe any nuclear morphological alteration that had occurred. As shown in Fig. 5B, the nuclei of cells from the untreated control group were mostly round in appearance and faintly stained (sample I). When GA and LPS were added together to the cells, the proportion of apoptotic nuclei (shrunken and intensely fluorescence-stained) increased substantially compared with the controls, and the ability of cells to adhere to acid slides

Fig. 5. Effects of GA on LPS-induced cell viability, apoptotic nuclear chromatin condensation, and stimulation of apoptosis-related caspase-3 activity in J774A.1 cells. A, effect of various doses of GA/LPS on cultured J774A.1 cell viability. Cells (5×10^5 cells/ml) were preincubated with various concentrations of GA (from 0.005 to 2 μM) for 1 h at 37°C, and then LPS or control buffer was added for a further 18 h in the presence of GA. After 2-h incubation with MTT (0.5 mg/ml), cells were lysed in acidic isopropanol (0.04–0.1 N HCl in absolute isopropanol), and the amount of MTT formazan was qualified by determining the absorbance at 570 nm via a microplate reader. B, DAPI staining for nuclear chromatin condensation of cell apoptosis. Cells were preincubated with GA (0.5 μM) for 1 h followed by LPS (1 μg/ml) treatment at the indicated times. At the end of LPS incubation, the attached cells on the glass slides were stained with DAPI. I, control; II, GA + LPS for 6 h; III, GA + LPS for 12 h; and IV, GA + LPS for 24 h. The insets to parts III and IV show the detailed views of nuclear chromatin condensation compared with I and II. The figures show representative experiments ($n = 3$). C, time-course study of effect of GA on LPS-induced caspase-3 activity. Cells were pretreated with GA (0.5 μM) for 1 h followed by incubation of LPS (1 μg/ml) for the indicated times as for 4, 8, and 12 h. At the end of treatments, an equal amount of cell lysate (50 μg of protein) from each sample was incubated in the presence of the caspase-3 fluorescence substrate, Ac-DEVD-AMC (50 μM), for 1 h at 30°C. Caspase-3 activity was measured fluorometrically after subtracting cleavage with excitation wavelength at 360 nm and emission wavelength at 460 nm, as described under *Materials and Methods*. Data are presented as fold of activated caspase-3 activity increase relative to the level of CTR (activity of control cells defined as 1). The data expressed are from one of four representative experiments and are expressed as mean ± S.E.

seemed to have decreased dramatically 24 h after GA and LPS exposure (Fig. 5B, samples II, III, and IV).

Because caspase-3 functions as an "executioner" in the apoptosis process (Hoshi et al., 1998; Condorelli et al., 2001), the enhanced caspase-3 activity reflects the increasing proportion of apoptotic cells in a tested sample. Hence, after incubation of cells with GA plus LPS for various times, caspase-3 activity was determined by measuring the degree of proteolytic cleavage of a particular fluorogenic substrate, Ac-DEVD-AMC. We observed that the caspase-3 activity of cells treated with GA plus LPS revealed a 16- and 24-fold increase in such activity at 8 and 12 h after treatment, respectively, compared with the corresponding control groups (Fig. 5C). In comparison, the incubation of cells with GA alone led to an increase in caspase-3 activity of approximately 5- (8 h) and 9-fold (12 h). Such results indicate that the combination of GA and LPS induced a greater level of cell apoptosis than was the case for either GA or LPS alone, revealing the role of Hsp90 regarding cell viability. Furthermore, we observed similar results that the caspase-9 activity of cells treated with GA plus LPS revealed a dramatic increase compared with the corresponding control groups (data not shown).

Involvement and Role of ROS (H_2O_2) in GA/LPS-Induced Apoptosis. It is considered by a number of researchers that ROS are toxic byproducts of aerobic metabolism, and a battery of studies have shown that ROS are able to activate caspases and trigger cell apoptosis (Azbill et al., 1997; Jacobson, 1997; Cesselli et al., 2001). As we have demonstrated above, the combination of GA with LPS (GA/LPS) quickly induces an enormous release of H_2O_2 (Fig. 4, A and B). Herein, we further investigated the molecular biological linkage between the GA/LPS combination-induced apoptosis and H_2O_2 activation. J774A.1 cells preincubated with NAC followed by exposure to the combination of GA and LPS, this treatment effectively blocked GA/LPS-induced H_2O_2 production (Fig. 4, A and B), and simultaneously decreased GA/LPS-stimulated caspase-3 activity by more than 80% compared with that of GA/LPS treatment alone (Fig. 6A). It is interesting to note that a similar role for H_2O_2 in GA/LPS-stimulated caspase-3 activity was seen for human blood monocyte-derived macrophages (Fig. 6B).

Furthermore, under microscopic examination, we observed a tremendous difference in cell morphology between GA/LPS-treated cells that had been pretreated with NAC and those that had not been exposed to such pretreatment (Fig. 6C). For example, in the absence of NAC-provided protection from GA/LPS-induced ROS, the normal morphology of cells featuring healthy round-shaped cells was not apparent; rather, cells seemed to have changed into irregular amoeba-shaped cells, a change which was also evidenced by multiple bledding in observed cells (Fig. 6C, samples IV versus I). In contrast, for the cells pretreated with NAC, the morphology of the majority of observed cells seemed to be much more similar to that of the control cells than was the case for cells not pretreated with NAC (Fig. 6C, samples V versus I). Clearly, a greater number of healthy-appearing cells were apparent after treatment with pre-NAC/GA + LPS than was the case after treatment with GA + LPS (i.e., no NAC pretreatment) even for as long as 15 h after GA/LPS exposure (Fig. 6C, samples V versus IV). In addition, the ability of cells to adhere to glass slides in the absence of NAC pretreatment before GA/LPS exposure seemed to be less substantial than was the case for cells pretreated with NAC. Taken together, these results indicate that GA/LPS-induced ROS production are involved in the activation of caspase-3 and suggest the relatively important role of Hsp90 regarding cell viability under LPS stimulation, a feature which, apparently, is directly related to apoptosis of the treated cells.

Discussion

Thus, we have demonstrated that LPS induces ROS release and transduces signals as part of the regulation of IL-1 gene expression of macrophages (Hsu and Wen, 2002). Using GA inhibition of Hsp90 function, we tested our hypothesis that GA-mediated Hsp90 plays an important role in the process of LPS-mediated cytokine regulation. Indeed, GA alters or blocks LPS activation of various signals in human macrophages and murine macrophages J774A.1, with such activation including LPS-induced Hsp90/Src heterocomplex formation, downstream activation and phosphorylation of MAPKs (Fig. 1), IL-1/pro-IL-1 expression (Fig. 2), TNF expression (data not shown), NF-κB activation (Fig. 3), and the release of ROS (Fig. 4). Herein, the effect of GA upon these reactions was observed in dose- and time-dependent fashions. In addition, Hsp90 directly participates in a battery of biological functions and properties relevant to the viability and cytotoxicity of LPS-treated macrophages (Fig. 7, A and B; see discussion below).

Our current findings have established that Hsp90 is involved in LPS-induced pp60Src complex formation and NF-κB activation; in addition, it modulates a series of LPS-mediated signaling molecules, which participate directly in the regulation of inflammatory cytokine pro-IL-1/IL-1 in macrophages (Fig. 7A). Specifically, Hsp90 in the LPS-induced p38 signaling pathway plays a more important role than would seem to be the case for the pathways involving JNK and ERK. GA reduces LPS-stimulated p38 phosphorylation to a basal level and partially reduces JNK phosphorylation (by approximately 30%) compared with LPS-treated cells (Fig. 1). In contrast, LPS stimulates ERK phosphorylation, albeit to a virtually insignificant level, although GA does reduce LPS-induced ERK phosphorylation to approximately 50% of the basal level. Moreover, Hsp90 acts with different roles and has an impact on the processes of IL-1 secretion, pro-IL-1 protein, and mRNA expression. For example, GA interferes with Hsp90 activity and completely inhibits its LPS-induced IL-1 secretion (Fig. 2A) and pro-IL-1 protein (Fig. 2B); however, GA blocks approximately 60% of LPS-induced pro-IL-1 mRNA (Fig. 2E). This suggests that Hsp90 plays a critical role in the post-translation and translation of IL-1/pro-IL-1 but a less-significant role in the transcription of the IL-1/pro-IL-1 message.

LPS activation of transcriptional factor NF-κB plays an important role in the regulation of a battery of macrophage inflammation-related genes such as IL-1 and TNF associated with immunity (Tak and Firestein, 2001; Zhang and Ghosh, 2001). Our current results indicate that GA decreases LPS-induced NF-κB activation (Fig. 3), which is similar to previous reports of LPS-dependent translocation of NF-κB into the impaired nucleus of GA-treated cells (Byrd et al., 1999; Vega and De Maio, 2003). Based on the current results of GA interference of LPS-induced NF-κB activation or transloca-

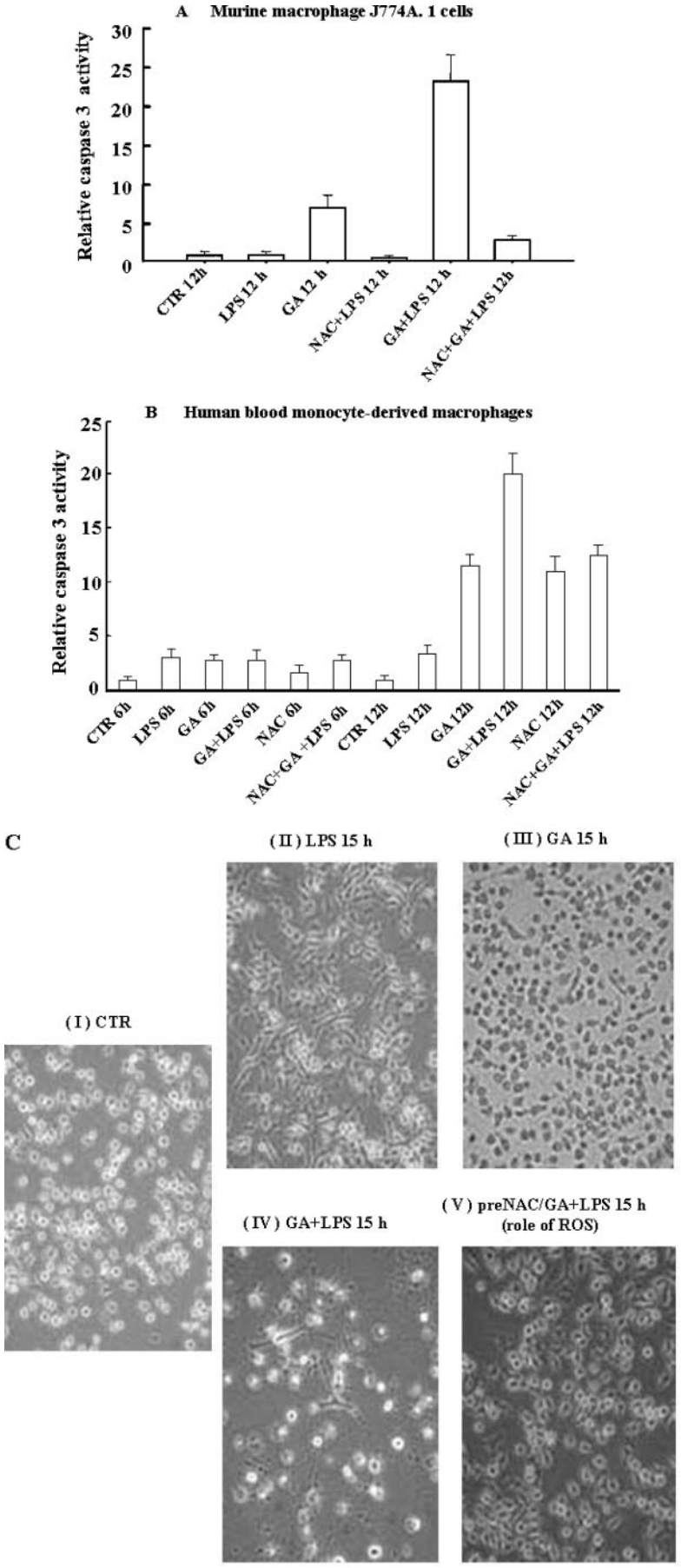

Fig. 6. Effects of GA/LPS-induced ROS on caspase-3 activity and apoptosis in both murine and human macrophages. A, role of ROS on GA/LPS-induced caspase-3 activity in murine macrophage J774A.1 cells. Cells were pretreated with or without NAC (10 mM) for 20 min followed by GA (0.5 μM) for 1 h before incubation of LPS (1 μg/ml) for an additional 12 h as indicated. At the end of LPS incubation, caspase-3 activity of treated cells was measured as described in Fig. 5. Data are presented as -fold of increased caspase-3 activity relative to the level of CTR (activity of control cells defined as 1). The data are representative of three similar experiments and are expressed as mean ± S.E. B, role of ROS on GA/LPS-induced caspase-3 activity in human blood monocytes-derived macrophages. The treatments and measurement of caspase-3 activity were basically similar to those described above (A), except that human macrophages and two LPS incubation periods of 6 and 12 h were used in the experiments. The data are representative of three similar experiments and are expressed as mean ± S.E. C, microscopic examination of apoptotic morphological changes in J774A.1 cells upon GA/LPS-induced ROS. Cells were preincubated with (preNAC) or without NAC as indicated and then treated with GA (0.5 μM) for 1 h, followed by additional 15 h LPS (1 μg/ml) incubation; then, the photomicrograph pictures were taken. I, control; II, LPS for 15 h; III, GA for 15 h; IV, GA + LPS for 15 h; and V, NAC pretreatment before GA+LPS challenge for 15 h. The figures are from one of four representative experiments (n = 4).

tion, we have elucidated the role of Hsp90 in the LPS-induced activation of NF-κB and of MAPKs in the regulation of gene expression of IL-1 and TNF (unpublished results). Hsp90, a chaperone protein, stabilizes its client proteins upon stress stimulation, and we have postulated another role for Hsp90 in NF-κB-mediated macrophage survival after LPS stimulation. Our results suggest that GA blocks LPS-induced NF-κB activation, most likely via the disruption of the interaction of Hsp90 and NF-κB or IκK (Nathan and Ding, 2001) or via another unidentified molecule X, which interacts with Hsp90 resulting in the destabilization of NF-κB or IκK and leading to apoptosis of macrophages (Fig. 5).

Several receptors on macrophages, including TLR4, CD14 (Medzhitov et al., 1997), and macrophage scavenger receptors (Hsu et al., 2001), interact with LPS and sequentially trigger various types of signal transduction. A recent finding suggests that GA inhibition of Hsp90 ameliorates the response to LPS for J774A.1 cells by decreasing CD14 surface expression via a rapid internalization of CD14 on cell membrane without any further replacement of CD14 (Vega and De Maio, 2003). We have demonstrated, however, that GA inhibition of LPS-induced IL-1 gene expression probably does not result from altering LPS binding and/or LPS-mediated signaling. It would seem to take approximately 16 h for GA impairment of LPS-dependent translocation of NF-κB to the nucleus to be realized and GA reduction of cell-surface expression of CD14 (Vega and De Maio, 2003). Comparing the mentioned GA reduction of CD14 expression with our tested reactions that took place within 1 to 2 h of LPS stimulation, the underlying mechanisms in a variety of reduction responses such as ROS production, NF-κB activation, MAPK activity, and pro-IL-1/IL-1 expression to LPS for GA-treated human macrophages or for J744A.1 cells probably are not related to the LPS-mediated reduction of CD14 surface expression, although we could not totally rule out the GA effect on CD14 as reported or effects of cross-talking between receptors of TLR4 or macrophage scavenger receptors. To elaborate the Hsp90 involvement in protein folding upon LPS binding to TLR4-mediated signal transduction, including interleukin-1 receptor-associated-kinase-1 (IRAK-1) protein, we found that pretreatment of J774A.1 cells with GA and LPS rapidly decreased IRAK-1 protein expression (data not shown). This finding was consistent with previous reports that GA inhibition of macrophage Hsp90 destabilizes and degrades IRAK-1 (De Nardo et al., 2005) and suggests the effect of LPS-induced Src/Hsp90 complex inhibition/disruption by GA on the stability of IRAK-1.

We further examined the role of Hsp90 for LPS-induced ROS, which relates to molecular/cellular characteristics of LPS-stimulated macrophages. Initially, from the minor ROS induction that arose from the internal GA control (Fig. 4), we ruled out the possibility of GA generating ROS via an Hsp90-independent mechanism, although GA did increase the level of ROS from macrophages compared with the control as

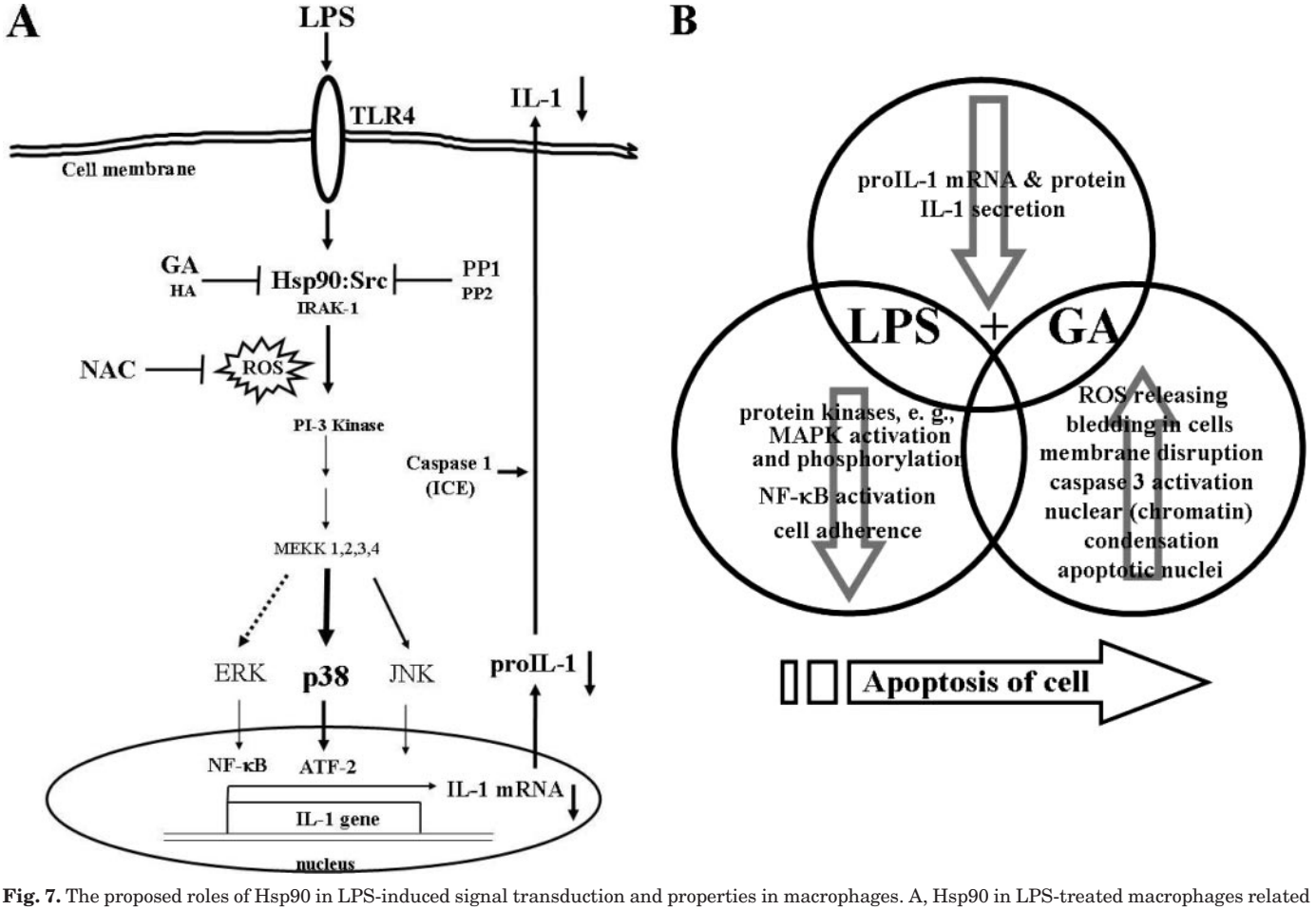

Fig. 7. The proposed roles of Hsp90 in LPS-induced signal transduction and properties in macrophages. A, Hsp90 in LPS-treated macrophages related to signaling of transcription and translation of IL-1/pro-IL-1; B. Hsp90 in LPS-stimulated macrophage relevant to viability and apoptosis.

reported previously (Dikalov et al., 2002; Lai et al., 2003). Our previous studies indicated that membrane-bound NADPH oxidase is one of the main sources of LPS-induced ROS (Hsu and Wen, 2002) and that pretreatment of macrophages with GA-enhancing LPS-induced ROS release is probably relevant to the activation of NADPH oxidase. NAC dramatically reduces GA/LPS-induced ROS production (Fig. 4), supporting the current evidence that GA disruption of Hsp90 mediated cellular functions. Specifically in this regard, we further examined the role of Hsp90 in the release of ROS and compared the cytotoxicity and viability of macrophages among LPS, GA, and a combination of LPS and GA, a cytotoxicity that presumably related to phagocytosis-associated ROS production. We have demonstrated the existence of the synergistic enhancement of cell apoptosis when GA was introduced in combination with LPS to cultured murine macrophages. Furthermore, we concluded this as evidenced by the observation of an enhanced proportion of apoptotic nuclei being present under macrophages incubated with LPS and GA (Figs. 5A) and of the simultaneous observation of the increasing slope of the caspase-3 activity curves (Fig. 5B); this is also the case for activation of caspase-9 (data not shown).

It has been documented that caspase-3 is sensitive to redox change and ROS expression for various tested cells (Ames et al., 1993; Manna and Aggarwal, 1999; Deshpande et al., 2000; Leroux et al., 2001). Indeed, NAC effectively abolishes ROS production, simultaneously inhibiting caspase-3 activation and reducing apoptosis, in that order, for GA-pretreated LPS-stimulated J774A.1 cells and for human macrophages, indicating that these reactions are species-independent. Considering the specific cytotoxicity of GA, we demonstrated that GA blocks the LPS-stimulated NF-κB activation at a GA concentration of 0.5 μM (Baldwin, 2001). On the other hand, with GA at a concentration of 5 μM, no inhibition of TNF-induced NF-κB was observed (data not shown), which suggests the existence of two completely different signal-transduction pathways. Such results exclude the possibility that GA may exert a direct cytotoxic effect on macrophages and act as a nonspecific inhibitor. Altogether, our results suggest that ROS play important roles in the process of GA plus LPS-induced cell apoptosis, indicating that Hsp90 modulates LPS-induced ROS release and further encourages macrophage apoptosis. Our current results demonstrate that Hsp90 plays a multifunction role for LPS-stimulated macrophages. Given that Hsp90 is abundant in the cytosol and that it can also be found on the membrane of macrophages, Nathan proposed that Hsp90 exerts cytokine-like effects on macrophages (Nathan and Ding, 2001).

In summary, based on the GA-specific inhibitory function of Hsp90 upon LPS stimulation of macrophages, we demonstrated the role of Hsp90 in LPS-induced ROS activation and illustrated the mechanism by which Hsp90 is involved in LPS-mediated signal transductions in the regulation of inflammatory cytokine IL-1 gene expression. Our results further elucidate Hsp90 regulation of pro-IL-1 production and of IL-1 secretion, which occur at multiple levels and which mainly involve the LPS-mediated activity of protein tyrosine kinase, including the phosphorylation and activation of protein kinase and the MAPKs (ERK, JNK, and p38) and activation of NF-κB. We analyzed the biological function of Hsp90 in injured macrophage cells relevant to apoptosis after exposure to LPS-induced ROS. We further demonstrated that GA interferes with the role of Hsp90 for LPS-treated macrophages by activation of caspase-3 activity, thus leading to apoptotic nuclear chromatin condensation. In contrast, NAC effectively blocks GA/LPS-induced ROS production, resulting in a rather dramatically decreased level of caspase-3 activity. The effect of pretreatment of macrophages with GA ameliorates the response of macrophages to LPS, implicating the role of Hsp90 in LPS stimulation (Vega and De Maio, 2003). Our current results establish the indispensable role of Hsp90 in the process of LPS-mediated immune signaling related to the tissue inflammatory process. It may indicate the potential for therapeutically applying GA to treat severe aberrant inflammatory responses for cases of multiorgan septic damage.

Acknowledgments

We gratefully acknowledge the anti-IL-1β, 3ZD monoclonal antibody, a gift from the National Institutes of Health (Bethesda, MD).

References

Ames BN, Shigenaga MK, and Hagen TM (1993) Oxidants, antioxidants, and the degenerative diseases of aging. *Proc Natl Acad Sci USA* **90:**7915–7922.

Azbill RD, Mu X, Bruce-Keller AJ, Mattson MP, and Springer JE (1997) Impaired mitochondria function, oxidative stress and altered antioxidant enzyme activities following traumatic spinal cord injury. *Brain Res* **765:**283–290.

Baldwin AS (2001) Control of oncogenesis and cancer therapy resistance by the transcription factor NF-kappaB. *J Clin Investig* **107:**241–246.

Billiet L, Furman C, Larigauderie G, Lariguderie G, Copin C, Brand K, Fruchart JC, and Rouis M (2005) Extracellular human thioredoxin-1 inhibits lipopolysaccharide-induced interleukin-1β expression in human monocyte-derived macrophages. *J Biol Chem* **280:**40310–40318.

Byrd CA, Bornmann W, Erdjument-Bromage H, Tempst P, Pavletich N, Rosen N, Nathan CF, and Ding A (1999) Heat shock protein 90 mediates macrophage activation by Taxol and bacterial lipopolysaccharide. *Proc Natl Acad Sci USA* **96:**5645–5650.

Cesselli D, Jakoniuk I, Barlucchi L, Beltrami AP, Hintze TH, Nadal-Ginard B, Kajstura J, Leri A, and Anversa P (2001) Oxidative stress-mediated cardiac cell death is a major determinant of ventricular dysfunction and failure in dog dilated cardiomyopathy. *Circ Res* **89:**279–286.

Chavany C, Mimnaugh E, Miller P, Bitton R, Nguyen P, Trepel J, Whitesell L, Schnur R, Moyer J, and Neckers L (1996) p185erbB2 binds to GRP94 in vivo. Dissociation of the p185erbB2/GRP94 heterocomplex by benzoquinone ansamycins precedes depletion of p185erbB2. *J Biol Chem* **271:**4974–4977.

Condorelli G, Roncarati R, Ross J, Pisani A Jr, Stassi G, Todaro M, Trocha S, Drusco A, Gu Y, Russo MA, et al. (2001) Heart-targeted overexpression of caspase3 in mice increases infarct size and depresses cardiac function. *Proc Natl Acad Sci USA* **9:**9977–9982.

DeBoer C, Meulman PA, Wnuk RJ, and Peterson DH (1970) Geldanamycin, a new antibiotic. *J Antibiot (Tokyo)* **23:**442–447.

Delude RL, Fenton MJR, Savedra R Jr, Perera PY, Vogel SN, Thieringer R, and Golenbock DT (1994) CD14-mediated translocation of nuclear factor-κB induced by lipopolysaccharide does not require tyrosine kinase activity. *J Biol Chem* **269:**22253–22260.

De Nardo D, Masendycz P, Ho S, Cross M, Fleetwood AJ, Reynolds EC, Hamilton JA, and Scholz GM (2005) A central role for the Hsp90-Cdc37 molecular chaperone module in interleukin-1 receptor-associated-kinase-dependent signaling by Toll-like receptors. *J Biol Chem* **280:**9813–9822.

Deshpande SS, Angkeow P, Huang J, Ozaki M, and Irani K (2000) Rac1 inhibits TNF-alpha-induced endothelial cell apoptosis: dual regulation by reactive oxygen species. *FASEB J* **14:**1705–1714.

Dikalov S, Landmesser U, and Harrison DG (2002) Geldanamycin leads to superoxide formation by enzymatic and non-enzymatic redox cycling. *J Biol Chem* **277:**25480–25485.

Gray JG, Chandra G, Clay WC, Stinnett SW, Haneline SA, Lorenz JJ, Patel IR, Wisely GB, Furdon PJ, and Taylor JD (1993) A CRE/ATF-like site in the upstream regulatory sequence of the human interleukin 1 beta gene is necessary for induction in U937 and THP-1 monocytic cell lines. *Mol Cell Biol* **13:**6678–6689.

Guha M and Mackman N (2001) LPS induction of gene expression in human monocytes. *Cell Signal* **13:**85–94.

Hoshi T, Sasano H, Kato K, Yabuki N, Ohara S, Konno R, Asaki S, Toyota T, Tateno H, and Nagura H (1998) Immunohistochemistry of caspase3/CPP32 in human stomach and its correlation with cell proliferation and apoptosis. *Anticancer Res* **18:**4347–4353.

Hsu HY, Chiu SL, Wen MH, Chen KY, and Hua KF (2001) Ligands of macrophage scavenger receptor induce cytokine expression via differential modulation of protein kinase signaling pathways. *J Biol Chem* **276:**28719–28730.

Hsu HY and Wen MH (2002) Lipopolysaccharide-mediated reactive oxygen species and signal transduction in the regulation of IL-1 gene expression. *J Biol Chem* **277:**22131–22139.

Jacobson MD, Weil M, and Raff MC (1997) Programmed cell death in animal development. *Cell* **88:**347–354.
Karin M (1995) The regulation of AP-1 activity by mitogen-activated protein kinases. *J Biol Chem* **270:**16483–16486.
Kim SO, Ono K, and Han J (2001) Apoptosis by pan-caspase inhibitors in lipopolysaccharide-activated macrophages. *Am J Physiol* **281:**L1095–L1105.
Lai MT, Huang KL, Chang WM, and Lai YK (2003) Geldanamycin induction of grp78 requires activation of reactive oxygen species via ER stress responsive elements in 9L rat brain tumor cells. *Cell Signal* **15:**585–595.
Leroux E, Auzenne E, Weidner D, Wu ZY, Donato NJ, and Klostergaard J (2001) Febrile and acute hyperthermia enhance TNF-induced necrosis of murine L929 fibrosarcoma cells via caspase-regulated production of reactive oxygen intermediates. *J Cell Physiol* **187:**256–263.
Malhotra V, Shanley TP, Pittet JF, Welch WJ, and Wong HR (2001) Geldanamycin inhibits NF-kappaB activation and interleukin-8 gene expression in cultured human respiratory epithelium. *Am J Respir Cell Mol Biol* **25:**92–97.
Manna SK and Aggarwal BB (1999) Lipopolysaccharide inhibits TNF-induced apoptosis: role of nuclear factor-kappaB activation and reactive oxygen intermediates. *J Immunol* **162:**1510–1518.
Mazia D, Schatten G, and Sale W (1975) Adhesion of cells to surfaces coated with polylysine. Applications to electron microscopy. *J Cell Biol* **66:**198–200.
Medzhitov R, Preston-Hurlburt P, and Janeway CA (1997) A human homologue of the *Drosophila* Toll protein signals activation of adaptive immunity. *Nature (Lond)* **388:**394–397.
Nagata S (1997) Apoptosis by death factor. *Cell* **88:**355–365.
Nathan C and Ding A (2001) TREM-1: a new regulator of innate immunity in sepsis syndrome. *Nat Med* **7:**530–532.
Richter K and Buchner J (2001) Hsp90: chaperoning signal transduction. *J Cell Physiol* **188:**281–290.
Tak PP and Firestein GS (2001) NF-kappaB: a key role in inflammatory diseases. *J Clin Investig* **107:**7–11.
Ulevitc RJ and Tobias PS (1995) Receptor-dependent mechanisms of cell stimulation by bacterial endotoxin. *Annu Rev Immunol* **13:**437–457.
Vega VL and De Maio A (2003) Geldanamycin treatment ameliorates the response to LPS in murine macrophages by decreasing CD14 surface expression. *Mol Biol Cell* **14:**764–773.
Wan CP, Myung E, and Lau BH (1993) An automated micro-fluorometric assay for monitoring oxidative burst activity of phagocytes. *J Immunol Methods* **159:**131–138.
Whitesell L, Mimnaugh EG, De Costa B, Myers CE, and Neckers LM (1994) Inhibition of heat shock protein HSP90-pp60v-src heteroprotein complex formation by benzoquinone ansamycins: essential role for stress proteins in oncogenic transformation. *Proc Natl Acad Sci USA* **91:**8324–8328.
Xu Y and Lindquist S (1993) Heat-shock protein hsp90 governs the activity of pp60v-src kinase. *Proc Natl Acad Sci USA* **90:**7074–7078.
Zhang G and Ghosh S (2001) Toll-like receptor-mediated NF-kappaB activation: a phylogenetically conserved paradigm in innate immunity. *J Clin Investig* **107:**13–19.

Address correspondence to: Dr. Hsien-Yeh Hsu, Department of Biotechnology and Laboratory Science in Medicine, National Yang-Ming University, 155 Li-Nong Street, Shih-Pai Taipei, Taiwan. E-mail: hyhsu@ym.edu.tw